Model-based Extraction of Input and Organ Functions in Dynamic Medical Imaging

Ondřej Tichý
Faculty of Nuclear Sciences and Physical Engineering, CTU in Prague, Czech Republic
Institute of Information Theory and Automation, Prague, Czech Republic

Václav Šmídl
Institute of Information Theory and Automation, Prague, Czech Republic

Martin Šámal
Department of Nuclear Medicine, 1st Faculty of Medicine, Prague, Czech Republic

ABSTRACT

Availability of input and organ functions is a prerequisite for analysis of dynamic image sequences in scintigraphy and positron emission tomography (PET) via kinetic models. This task is typically done manually by a human operator who may be unreliable. We propose a probabilistic model based on physiological assumption that time-activity curves (TACs) arise as a convolution of an input function and organ-specific kernels. The model is solved via the Variational Bayes estimation procedure and provides estimates of the organ images, the TACs, and the input function as results. The ability of the resulting algorithm to extract the input function is tested on data from dynamic renal scintigraphy. The estimated input function was compared with the common estimate based on manual selection of the heart ROI. The method was applied to the problem of relative renal function estimation and the results are compared with competing techniques. Results of comparison on a dataset of 99 patients demonstrate usefulness of the proposed method.

Keywords: dynamic medical imaging, compartment modeling, convolution, blind source separation

1 INTRODUCTION

Decomposition of the observed sequences of images into tissue images and their associated time-activity curves (TACs) is a common task in nuclear medicine in scintigraphy or positron emission tomography (PET). The knowledge of the input function is often necessary for further analysis [15]. For example, the input function is essential in the Patlak-Rutland plot [12]. In PET, the input function can be directly measured by sampling the arterial blood [8]. This approach needs a medical intervention which is often not appropriate in clinical practice. This invasive procedure can be substituted by extraction of the input function from the observed images using manual selection of regions of interest (ROIs) in the observed images. It can be placed directly on the heart, if available, or on other vascular structures if they can be recognized on the images [7]. The disadvantages of manual selection of the ROIs are substantial: the position of ROIs is strongly operator-dependent and very time-consuming [3, 4]. Moreover, it is possible that the selected ROI does not contain only the vascular activity but also other tissues in the background.

Automatic, or semi-automatic methods for ROI selection are available [6], however, they are not completely reliable and the activity is always counted from the full area of ROI which may still include some background organs. An alternative approach is to use some blind source separation method (BSS). They have no physiological assumption in their basic form, [11], however, some extensions have also been proposed [5, 13]. We design a mathematical model that integrates all common assumption of the domain, including convolution of the input function and tissue-specific kernels. The input function as well as the kernel parameters are considered to be unknown. They are estimated from the observed images using the Variational Bayes method [16].

The proposed method is used to create a semi-automated procedure for estimation of relative renal function. Suitability of the procedure is studied on a dataset of 99 patients [1]. For comparison, the same data were analyzed using manual ROI placement by an expert and by a trained novice as well as the state of the art algorithm of blind source separation [11]. We show that the results of the proposed model are closer to those of the experienced expert that results of any other competing methods. Joint estimation of the input function is thus the key improvement of the

blind source separation approach for this task.

2 METHOD

The goal of the designed method is to automatically identify tissue structures and their related time-activity curves (TACs) from the observed sequence of images. Estimation procedure is based on probabilistic model that is designed using common assumptions used in nuclear medicine. These assumptions are: (i) the observed image is a superposition of the underlying tissue images; (ii) the time activity curves are described by compartment model, where each time-activity curve arise as a convolution between a common input function and a tissue-specific kernel [13]; (iii) the tissue images and the time activity curves are non-negative; and (iv) the variance of the observation noise is proportional to the signal strength. These assumption are now formulated mathematically via a probabilistic model. The Variational Bayes methodology is used to estimate all unknown parameters of the proposed model.

2.1 *Mathematical Model Assumptions*

The observed sequence of images is indexed by a discrete time index t, the number of images in the sequence is n. The sequence is assumed to be composed of r underlying tissues indexed by symbol $f = 1, \ldots, r$, r is unknown. Each observed image is stored in one vector $\mathbf{d}_t$ with the pixels stored columnwise and is assumed to be a sum of contributions from the underlying tissues

$$\mathbf{d}_t = \sum_{f=1}^{r} \mathbf{a}_f x_{t,f}, \tag{1}$$

where $\mathbf{a}_f$ are the tissue image in the same vector form as the observed image, and $x_{t,f}$ is the activity of the fth tissue at time t. The time-activity curve $\mathbf{x}_f$, i.e. the organ function, is supposed to be the result of convolution of the common input function, $\mathbf{b}$, and a tissue-specific kernel, $\mathbf{u}_f$. The tissue-specific kernels, $\mathbf{u}_f$ are modeled using increments $\mathbf{w}_f$ as suggested in [10], hence

$$x_{t,f} = \sum_{i=1}^{t} b_{t-i+1} u_{i,f}, \tag{2}$$

$$u_{t,f} = \sum_{i=t}^{n} w_{i,f}, \tag{3}$$

and $w_{i,f} = \begin{cases} h_f & s_f \leq t \leq s_f + l_f \\ 0 & \text{otherwise,} \end{cases}$. Here, $\mathbf{w}_f$ is the fth tissue-specific vector with non-negative elements with specified structure. Here, h_f is the height of each increment in fth tissue, s_f is the starting point of the increments and $s_f + l_f$ is the ending point of the increments. In other words, the vector $\mathbf{w}_f$ is supposed to be in the form of $[0, \ldots, 0, h_f, \ldots, h_f, 0, \ldots, 0] \equiv M_{w_f}$.

The input function $\mathbf{b}$ is also modeled incrementally as

$$b_t = \sum_{i=t}^{n} g_i. \tag{4}$$

2.2 *Probabilistic Model*

The deterministic model assumptions in Section 2.1 are valid only approximately. For example, the measurements of $\mathbf{d}_t$ (1) are subject to noise with unknown variance ω. The observed images $\mathbf{d}_t$ are thus random realizations from the probability density:

$$f(\mathbf{d}_t|\omega) = \text{tN}(\sum_{f=1}^{r} \mathbf{a}_f x_{t,f}, \omega^{-1} I_p), \tag{5}$$

$$f(\omega) = \text{G}(\vartheta_0, \rho_0), \tag{6}$$

where p denotes the number of pixels in the image, I_n is the identity matrix of size n, $\text{tN}(.,.)$ is the multivariate normal distribution truncated to positive values with given mean vector and covariance matrix. Following the Bayesian approach, each unknown parameter needs to have a prior distribution of its potential values. The prior distribution of the unknown variance of the observation noise, ω, is assumed to be of the gamma form with prior parameters ϑ_0, ρ_0.

The convolution kernel (2) may also differ from the assumed form, where variances of the differences $\mathbf{w}_f$ are unknown, denoted ξ_f . The model of the TACs is composed from the kernels $\mathbf{w}_f$ and the input function $\mathbf{b}$. The prior distribution of the fth TAC model is then

$$f(\mathbf{w}_f|\xi_f) = \text{tN}(M_{w_f}, \xi_f I_n), \tag{7}$$

$$f(\xi_f) = \text{G}(\kappa_{f,0}, \nu_{f,0}), \tag{8}$$

and $f(h_f) = \text{tN}(\mathbf{0}_{r\times 1}, \tau_0)$, $f(l_f|s_f) = \text{U}(0, n - s_f)$, and $f(s_f) = \text{U}(0, n)$, where the parameters indexed with zero are assumed to be known prior parameters, and $\text{U}(.,.)$ is the uniform distribution.

The differences between the true input function and the model of increments of the blood, $\mathbf{g}$, are assumed to have an unknown variance ψ. The prior distributions for the parameters of the input function and the tissue images are:

$$f(\mathbf{g}|\psi) = \text{tN}(\mathbf{0}_{n\times 1}, \psi^{-1} I_n), \tag{9}$$

$$f(\mathbf{a}_f|\upsilon_f) = \text{tN}(\mathbf{0}_{p\times 1}, \upsilon_f^{-1} I_p), \tag{10}$$

$$f(\psi) = \text{G}(\zeta_0, \eta_0), \tag{11}$$

$$f(\upsilon_f) = \text{G}(\alpha_{f,0}, \beta_{f,0}). \tag{12}$$

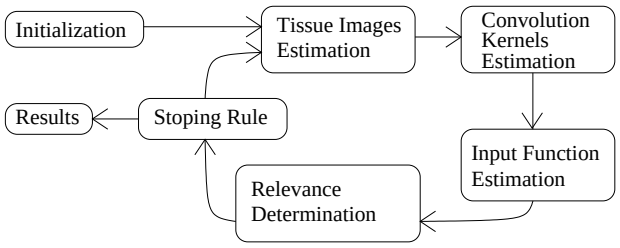

Figure 1: The computation scheme of the BCMS algorithm.

Here, υ_f is a hyperparameter that allows to select the number of relevant tissue images, r, via the automatic relevance determination approach (ARD), [2].

In further text, this model will be denoted as the Blind Compartment Model Separation (BCMS).

2.3 *Variational Bayes Solution*

Variational Bayes method, [16, 11], is a technique for assesment of shapping parameters θ of posterior distribution $f(\theta|D)$. A parametric probabilistic model of the observation is given as $f(D|\theta)$, data D is conditioned by multivariate parametr $\theta = [\theta_1, \ldots, \theta_q]'$. The task is to find out a distribution $\tilde{f}(\theta|D)$ which should be as close as possible to the true posterior distribution $f(\theta|D)$. Formally,

$$\tilde{f}(\theta|D) = \arg\min_{\breve{f}\in\mathbf{F}_c} \Delta\left(\breve{f}(\theta|D)||f(\theta|D)\right), \quad (13)$$

where $\Delta(f||g)$ is a meassure between functions f and g and $\mathbf{F}_c$ is the space of conditionally independent functions. The Variational Bayes method selects as the meassure the Kullback-Leibler divergence (KLD) [9], i.e. $\Delta \equiv$ KLD, which is defined as

$$\mathrm{KLD}\left(\breve{f}(\theta|D)||f(\theta|D)\right) = \int \breve{f}(\theta|D) \ln \frac{\breve{f}(\theta|D)}{f(\theta|D)} \mathrm{d}\theta. \quad (14)$$

Then, the shapping parameters of posterior distribution can be found using the Variational Bayes theorem:

$$\tilde{f}(\theta_i|D) \propto \exp\left(\mathrm{E}_{\tilde{f}(\theta_{/i}|D)}\left[\ln\left(f(\theta, D)\right)\right]\right), \quad i = 1, \ldots, q, \quad (15)$$

where symbol $\propto$ means up to normalizing constant, $\mathrm{E}_f(.)$ means expected value of an argument with respect to distribution f, and $\theta_{/i}$ denotes complement of θ_i in θ; hence, $\theta_{/i} = [\theta_1, \ldots, \theta_{i-1}, \theta_{i+1}, \ldots, \theta_q]$.

Following the Variational Bayes method, we build the joint density and seek its approximation in the form of conditionally independent posteriors. The equations form an implicit set that needs to be solved iteratively. The computation scheme is shown in Fig. 1. Each experiment runs till the hyperparameters υ_f are stabilized. The details are given in Research Report [14].

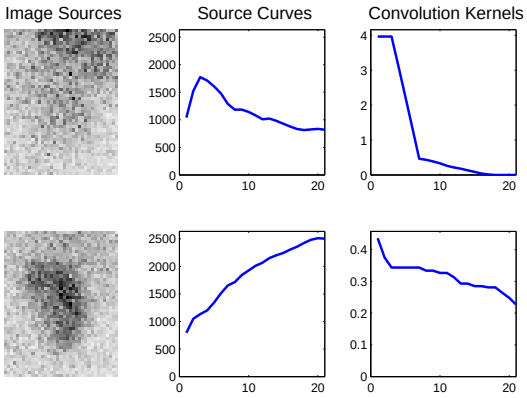

Figure 3: Estimates provided by the BCMS algorithm for a selected data set, right ROI. **Left**: estimated tissue images; **middle**: estimated time-activity curve; **right**: estimated tissue-specific kernel.

3 RESULTS

The iterative algorithm was tested on a dataset from renal scintigraphy, [1]. The full database contains 99 patients with both kidneys where relative renal function (RRF) could be estimated. Each study contains 180 images of 128×128 pixels recorded in 10 seconds interval. The RRF is traditionally computed on the uptake part of the sequence, i.e. the interval when the kidney only accumulates the activity without secretion and only the parenchyma-part of the kidney is activated. The parenchyma is the spongy tissue covering the whole kidney which accumulates the activity from the blood. Detection of the uptake time is manual and the same part is used for all compared methods.

First, we demonstrate the output of the BCMS model, i.e. the estimates of the input and organ functions, on selected sequences. Second, we apply the BCMS model for estimation of the RRF and provide statistical comparison to competing methods.

3.1 *Input and Organ Functions Estimation*

The BCMS algorithm is applied on a rectangular ROIs with left and right kidney. The BCMS algorithm provides results in the form of tissue images, $\mathbf{a}_f$, tissue-specific convolution kernel, $\mathbf{u}_f$, and input function, $\mathbf{b}$, see Figure 3 for results on the right kidney from the sequence in Figure 2 as an example. The ARD property of the algorithm selected two structures to be relevant which corresponds well with biological assumptions. The estimates corresponding to the background are displayed in the first row, those corresponding to the parenchyma in the second row. The estimated input function of this dataset is displayed in Figure 4 left.

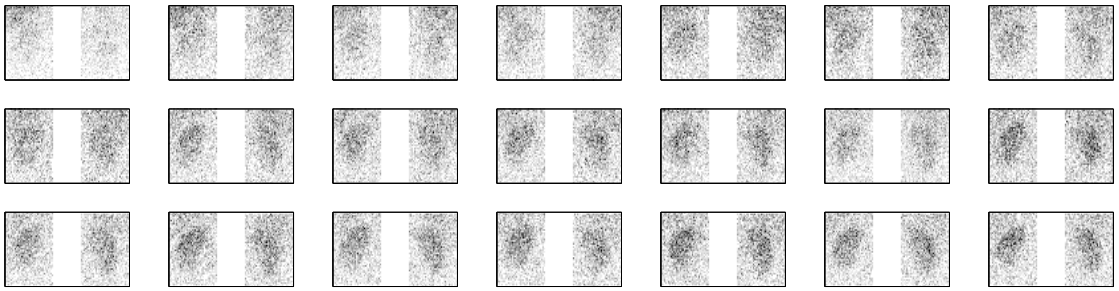

Figure 2: The uptake part of the scintigraphic sequence. It can be seen rough placed rectangular ROIs on left and right kidneys.

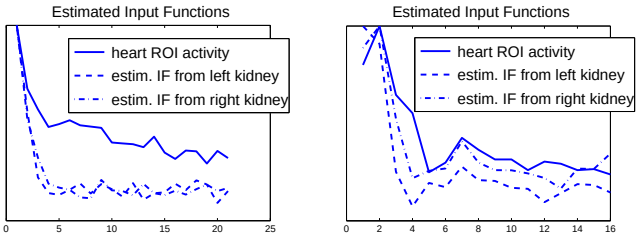

Figure 4: Estimated input functions (IF) from two selected sequences.

Since the ground truth is not available and the input function is usually associated with the blood activity, we compare estimated input functions from both ROIs with the activity computed from a manually selected ROI of the heart. The left and right rectangular ROI do not overlap, yet the estimates of input functions correspond well to each other. Note that the estimated input function decays much faster than the activity in the heart ROI in this study. This is caused by the presence of lungs in the ROI. In Figure 4, right, the same estimates for another dataset are displayed. In this case, the estimates of the input function corresponds well with the recorded activity in the heart ROI. We conjecture that in this case, the ROI contained only the heart and not other tissues.

3.2 *Relative Renal Function Estimation*

Relative renal function is mathematically simple but clinically important and hardly obtainable parameter. It is defined as:

$$RRF = \frac{L_p}{L_p + R_p}, \tag{16}$$

where L_p, is the total activity of the left parenchyma (i.e. one of the tissue from decomposition (1)), and R_p is the total activity in the right parenchyma.

In this Section, four methods are applied to the data set and their results are compared, two manual and two semi-automatic.

(i) Reference Manual Method (**RMM**): The assessment of RRF is typically based on manual drawing of the Regions of Interest (ROIs) of parenchyma, however, details of subsequent evaluation differ from one hospital to another [4, 3]. The studied data set already provides results of the RRF analysis obtained by a experienced physician using a range of methods including the Patlak-Rutland plot, [12], crosschecking with the deconvolution method [10].

(ii) Straightforward Manual Method (**SMM**): Is an example of another commonly used approach. Four ROIs are manually drawn for each data set, in our case by a trained novice. These are: the left and the right kidney, and the left and the right backgrounds on the outer side of the kidneys. The activity of the reference backgrounds are subtracted from the activity in the related kidneys. It is assumed that the same background is behind (or in front of) the kidney.

(iii) Semi-automatic BCMS-based Method (**BCMS**): The operator is asked to position two rectangular ROI around each kidney. The BCMS is applied to each of these rectangular ROIs to obtain estimates of two underlying structures (as demonstrated in Figure 3). The estimate of the parenchyma images is thresholded at $0.5\times$maximum of the image to remove remaining traces of the background.

(iv) Common Blind Source Separation Method (**BSS**): The task of decomposition of the observed data into a superposition of a product of two unknowns (equation (1)) has been studied in the blind source separation literature. Specifically, the method described in [11] is based on the same assumptions as the proposed BCMS except for the convolution model. Comparison with this method then allows to study the influence of this modeling choice to the results.

Statistical Comparison

The four described methods will be compared via difference of their results of RRF from those provided by the experienced expert (RMM) as a reference value. Since the expert considered all assumptions of the approach in his evaluation, we will consider the automatic method that is closer to his results to be better. The differences were computed for all 99 patients and the results are displayed in Table 1 via quantiles. Note that the estimates of the BCMS method are systematically closer to the reference values than those of the competing methods. The computation time of the semi-automatic methods (iii) and (iv) is comparable, one sequence is processed under one minute.

Table 1: Quantiles of the difference of the estimated RRF from the reference value for all 99 patients.

method	<5%	<10%	≧10%
BSS	39.6%	82.2%	18.8%
SMM	36.5%	70.8%	29.2%
BCMS	63.5%	89.6%	10.4%

Table 2: Quantiles of the difference of the estimated RRF from the reference value for the patients with diagnosed abnormality in kidney function.

method	<5%	<10%	≧10%
BSS	39.1%	69.6%	30.4%
SMM	17.4%	47.8%	52.2%
BCMS	58.7%	80.4%	19.6%

The results for the patients with diagnosed abnormality in kidney function are shown in Table 2. There is significantly lower signal, hence, the spread of the errors is much higher. However, the relative performance of the compared methods is the same on both data sets, with BCMS being the closest to the references.

4 DISCUSSION

The proposed BCMS method is able to provide both the input function and the organ function. The results presented in Fig. 4 suggest that the estimated input function differs from the activity curve in the heart ROI which is considered to be its reliable estimate. While it is possible to explain this discrepancy by the background tissue, it is also possible that the estimate is only local minima in the space of possible solutions. Or the model assumption may not be appropriate for the given patient. A dataset that would also have the input function measured by blood sampling would be necessary to resolve this issue.

The presented semi-automatic method of RRF analysis was run with manual intervention in two key steps: (i) positioning of the rectangular ROIs to contain the left and right kidney, and (ii) selection of the uptake part of the sequence. While the first step is relatively easy to automate and seldom requires intervention, the second step is more demanding. Specifically, we select the uptake part to start at the peak of the vascular activity in the ROI of the kidney. The end of the sequence is determined by the peak of the parenchyma activity. More detailed modeling of the sequence is needed to achieve fully automated method.

5 CONCLUSION

A probabilistic model of medical image sequences and its Variational Bayesian solution for functional analysis of medical data was proposed. Time activity curves are modeled as convolution of an unknown input function with kernels. The shape of each kernel is restricted to match the biological assumptions used in compartment modeling. The resulting algorithm thus achieves blind separation of compartment models with common input function. No manual intervention is required in this process. We have shown that the estimated input and organ functions correspond well with the biological expectations. Since the method does not use any modality-specific assumptions it can be used in any other modality.

The algorithm was further applied to semi-automatic analysis of relative renal function from scintigraphic data. Manual intervention was required to select the uptake part of the sequence and the position of the rectangular areas containing the left and the right kidney. The results were compared to two completely manual methods and a common blind source separation method with the same level of intervention. The most sophisticated manual method performed by an experienced expert was selected as a reference value. On a dataset of 99 patients, the estimates provided by the proposed method were found to be systematically closer to the reference value than those of any other method.

Acknowledgment
This work was supported by the Grant Agency of the Czech Technical University in Prague, grant No. SGS11/162/OHK4/3T/14 and by the Czech Science Foundation, grant No. 13-29225S.

REFERENCES

[1] Database of dynamic renal scintigraphy - www.dynamicrenalstudy.org.

[2] C.M. Bishop and M.E. Tipping. Variational relevance vector machines. In *Proceedings of the 16th Conference on Uncertainty in Artificial Intelligence*, pages 46–53, 2000.

[3] A. Brink, M. Šámal, and M.D. Mann. The reproducibility of measurements of differential renal function in paediatric 99mtc-mag3 renography. *Nuclear medicine communications*, 33(8):824–831, 2012.

[4] M. Caglar, G.K. Gedik, and E. Karabulut. Differential renal function estimation by dynamic renal scintigraphy: influence of background definition and radiopharmaceutical. *Nuclear medicine communications*, 29(11):1002, 2008.

[5] L. Chen, P.L. Choyke, T.H. Chan, C.Y. Chi, G. Wang, and Y. Wang. Tissue-specific compartmental analysis for dynamic contrast-enhanced mr imaging of complex tumors. *IEEE Transactions on Medical Imaging*, 30(12):2044–2058, 2011.

[6] E.V. Garcia, R. Folks, S. Pak, and A. Taylor. Totally automatic definition of renal regions-of-interest from tc-99m mag3 renograms: Validation in patients with normal kidneys and in patients with suspected renal obstruction. *Nuclear medicine communications*, 31(5):366, 2010.

[7] G. Germano, B.C. Chen, et al. Use of the abdominal aorta for arterial input function determination in hepatic and renal pet studies. *Journal of nuclear medicine*, 33(4):613, 1992.

[8] H.N.J.M. Greuter, R. Boellaard, et al. Measurement of 18f-fdg concentrations in blood samples: comparison of direct calibration and standard solution methods. *Journal of nuclear medicine technology*, 31(4):206–209, 2003.

[9] S. Kullback and R.A. Leibler. On information and sufficiency. *Annals of Mathematical Statistics*, 22(1):79–86, 1951.

[10] A. Kuruc, JH Caldicott, and S. Treves. Improved Deconvolution Technique for the Calculation of Renal Retention Functions. *COMP. AND BIOMED. RES.*, 15(1):46–56, 1982.

[11] J.W. Miskin. *Ensemble learning for independent component analysis*. PhD thesis, University of Cambridge, 2000.

[12] C.S. Patlak, R.G. Blasberg, J.D. Fenstermacher, et al. Graphical evaluation of blood-to-brain transfer constants from multiple-time uptake data. *J Cereb Blood Flow Metab*, 3(1):1–7, 1983.

[13] D.Y. Riabkov and E.V.R. Di Bella. Estimation of kinetic parameters without input functions: analysis of three methods for multichannel blind identification. *Biomedical Engineering, IEEE Transactions on*, 49(11):1318–1327, 2002.

[14] O. Tichý and V. Šmídl. Convolution Model of Time-activity Curves in Blind Source Separation. Technical Report 2330, UTIA, 2013.

[15] D. Vriens, L.F. de Geus-Oei, W.J.G. Oyen, and E.P. Visser. A curve-fitting approach to estimate the arterial plasma input function for the assessment of glucose metabolic rate and response to treatment. *Journal of Nuclear Medicine*, 50(12):1933–1939, 2009.

[16] V. Šmídl and A. Quinn. *The Variational Bayes Method in Signal Processing*. Springer, 2006.